Can. J. Remote Sensing, Vol. 36, No. 5, pp. 464–473, 2010

Radiometric intercomparison of AATSR, MERIS, and Aqua MODIS over Dome Concordia (Antarctica)

Marc Bouvet and Fabrizio Ramoino

Abstract. The Advanced Along-Track Scanning Radiometer (AATSR), Aqua Moderate Resolution Imaging Spectroradiometer (A-MODIS), and Medium Resolution Imaging Spectrometer (MERIS) level 1 data are compared at top-of-atmosphere level for nearly simultaneous observations carried out under nearly identical geometries. Comparisons are carried out over Dome Concordia, on the Antarctic Plateau. When comparing the radiometry of these sensors over this site, we estimate the systematic uncertainty of this methodology to be less than 3% and the random uncertainty to be about 2%. This methodology indicates that MERIS and A-MODIS bands at about 560 and 860 nm are in radiometric agreement within the systematic uncertainty of the methodology. AATSR seems to be in line with the two previous sensors at 560 and 670 nm, but differences of 4% are measured at 860 nm.

Résumé. On compare les données d'AATSR (« Advanced Along-Track Scanning Radiometer »), de MODIS (« Moderate Resolution Imaging Spectroradiometer ») – Aqua et de MERIS (« Medium Resolution Imaging Spectrometer ») de niveau 1 acquises au niveau du sommet de l'atmosphère pour des observations quasi simultanées effectuées dans des conditions de géométrie presque identiques. Les comparaisons ont été réalisées au-dessus du Dôme Concordia, sur le plateau antarctique. On évalue l'incertitude systématique de cette méthodologie dans la comparaison de la radiométrie de ces capteurs au-dessus de ce site à moins de 3 % et l'incertitude aléatoire à environ 2 %. Cette méthodologie montre que les bandes de MERIS et de A-MODIS à environ 560 et 860 nm concordent au plan radiométrique avec l'incertitude systématique de la méthodologie. AATSR semble s'orienter dans le même sens que les deux capteurs précédents à 560 et 670 nm, bien que l'on observe des différences de 4 % à 860 nm.
[Traduit par la Rédaction]

Introduction

With emerging large-scale initiatives involving more space agencies and member states, such as the Global Earth Observation System of Systems (GEOSS), the need for interoperability, data merging, and data continuity is growing. To effectively monitor the Earth from space, it is essential that the multitude of observations made by space sensors be made consistent. Ensuring that the calibration differences between sensors are understood and well quantified is an essential step in the implementation of a long-term global monitoring plan.

A variety of vicarious calibration methodologies have been developed for sensors observing the Earth in the sun-reflected part of the electromagnetic spectrum. All the methodologies eventually rely on the transfer of a radiometric standard between two instruments.

A first broad category of calibration methodology relies on radiative transfer simulations. To accurately predict the top-of-atmosphere (TOA) signal measured by a satellite sensor with a radiative transfer model, one generally needs to measure or assume the following inputs: (1) the surface bidirectional reflectance distribution function (BRDF), (2) the aerosol optical properties (scattering and absorption) and their vertical distribution, (3) the concentration profile of absorbing gases (e.g., O_3, H_2O, O_2, NO_2), and (4) temperature and pressure profiles. If all atmospheric and surface measurements are traceable to the International System of Units (SI), the space measurements can be calibrated in absolute terms against simulated TOA measurements. In practice, setting up and maintaining a comprehensive field experiment to perform these measurements is difficult, and thus assumptions are made about the surface or atmospheric properties (e.g., Lambertian BRDF, standard atmospheric gases concentration, and standard atmospheric pressure and temperature profiles). The radiative transfer modelling is also often approximated (e.g., scalar radiative transfer equation solving, plane parallel atmosphere assumption, and correlated *k* distribution atmospheric absorption coefficients). Examples of such an approach, where both surface and atmospheric optical properties are measured, can be categorized in the so-called reflectance-based approach (see, for instance, its application to the Landsat series in

Received 24 February 2010. Accepted 26 August 2010. Published on the Web at http://pubservices.nrc-cnrc.ca/cjrs on 25 March 2011.

M. Bouvet[1] and F. Ramoino. European Space Agency – European Space Research and Technology Centre (ESA/ESTEC), Keplerlaan 1, PB 299, NL-2200 AG Noordwijk, The Netherlands.

[1]Corresponding author (e-mail: marc.bouvet@esa.int).

Thome, 2004). Methodologies based on radiative transfer modelling can also be applied when surface and atmospheric measurements are not available; Vermote et al. (1992) demonstrates that observation over oceanic sites can be simulated to within 5% in specific conditions. The methodology described in Cabot et al. (1999) and used operationally by the Centre national d'études spatiales (CNES) over pseudo-invariant desert sites, selected for their spatial homogeneity and stability in time, is another example where no in situ data are used to predict the TOA signal. The first step in this methodology is to identify pairs of acquisitions between a given acquisition from a space sensor to be calibrated and the full archive of acquisitions from a reference space sensor that are made under the same observational geometry (acquisitions between the two sensors are thus generally not concomitant and can be separated by years). Then, starting from the TOA signal measured by the reference sensor, an atmospheric correction is performed to retrieve the surface reflectance, and after spectral interpolation to the spectral response of the other sensor, the atmospheric contribution is added to simulate the TOA signal measured by the sensor to be calibrated.

The previously mentioned methodologies rely on atmospheric correction. An alternative to radiative transfer modelling for the purpose of vicarious calibration can be found in Smith et al. (2008), where the temporal radiometric stability is assessed for several space sensors using measurements over pseudostable terrestrial sites and by correcting for TOA BRDF effects using a polynomial fit of the TOA reflectance as a function of the scattering angle. It important to stress that no atmospheric correction is necessary in this approach, allowing for the identification of long-term drifts.

Another way to transfer (or compare) measurements between two space sensors at TOA measurement level is to view the same target, at the same time, under the same viewing geometry, and in identical spectral bands. Such direct comparison also removes the need for in situ measurements and radiative transfer forward or inverse modelling (and the associated assumptions and uncertainties). Cao et al. (2004) developed an approach to identify and exploit these observations (the so-called Simultaneous Nadir Overpass (SNO)). The intrinsic limitation ofthe Cao et al. methodology is that only nadir observations can be compared, and thus the entire field of view of an imaging instrument cannot be characterized. Moreover, this methodology is restricted to the observation of high-latitude targets (about 10° to the poles). We present in this paper an alternative methodology also aiming at identifying directly comparable TOA observations from two sensors, and we demonstrate this approach at a high-latitude terrestrial site. Such an approach was also applied by Bouvet (2006) at low-latitude sites (about 20°S) such as the Salar of Uyuni, Bolivia. We apply this methodology to data from the Medium Resolution Imaging Spectrometer (MERIS) and the Advanced Along-Track Scanning Radiometer (AATSR), both on the ENVISAT platform, and the Moderate Resolution Imaging Spectroradiometer onboard the Aqua platform (A-MODIS). Because all three missions share similarities, their data are naturally inclined to be compared or merged. AATSR, A-MODIS, and MERIS all possess onboard calibration devices characterized prior to their launch and traced to SI units. These devices are operationally used to monitor and correct for sensor degradation. Therefore, the sensors have an onboard absolute calibration device. In addition, vicarious calibration methodologies are used as an alternative to the onboard calibration techniques of these sensors (Tinel, 2006; Smith et al., 2008; Xiong et al., 2003).

In this study we attempt to characterize the relative differences in radiometric calibration between AATSR, A-MODIS, and MERIS. The natural terrestrial target chosen for this intercomparison is Dome Concordia in Antarctica (Dome C), one of the sites identified by the Committee on Earth Observation Satellites (CEOS) as one of the LANDNET sites (i.e., standard reference sites for the postlaunch calibration of space-based optical imaging sensors).

In the first part of this paper we present our methodology, which is based on the identification of directly comparable near-simultaneous TOA reflectance measurements from two space sensors made under similar observational geometries. Similarly to the SNO methodology, neither atmospheric nor BRDF correction is required to radiometrically compare two sensors. We then discuss Dome C characteristics and climatology, followed by a description of the remote sensing data and the results of the radiometric intercomparison and a discussion on the sources of radiometric differences between sensors and on methodological uncertainties.

Methodology

The objective of the methodology can be summarized as follows: identify radiometric calibration differences between two sensors by comparing their observations made over the same terrestrial target, at TOA, at the same time, and under the same geometrical configuration.

First, level 1B (L1B) data from AATSR, A-MODIS, and MERIS in all available bands spanning from 400 to 1020 nm are systematically extracted over the same region of interest (ROI). These data are then cloud screened. Because an automatic cloud screening based on radiometry for Dome C is difficult to achieve (owing to the similar spectral signature of clouds and snow in the visible range and the high altitude of the plateau), all data were visually cloud screened.The data were then converted into remote sensing reflectance:

$$\rho^{\mathrm{TOA}} = \frac{\pi L^{\mathrm{TOA}}}{E_0 \cos(\mathrm{SZA})} \tag{1}$$

where L^{TOA} is the TOA spectral radiance, E_0 is the extraterrestrial solar irradiance at a given date (i.e., corrected for the Earth–Sun distance), and SZA is the sun zenith angle.

This conversion is carried out using the extraterrestrial spectral irradiance spectrum specific to each mission and the relative spectral responses (RSRs) of each band from each instrument as provided by the respective space agencies.

For each acquisition from each sensor, the following parameters are archived: the reflectances in all spectral bands, the SZA, the viewing zenith angle (VZA), and the viewing azimuth angle relative to the principal plane (RAA). These parameters are averaged over all pixels included in a predefined ROI several tens of square kilometres in size.

Occurrences of concomitant observations by two sensors, i and j, under nearly identical geometries of observation and illumination are searched. We henceforth call such occurrences doublets. To minimize differences due to temporal surface reflectance changes, doublets are considered valid only if the observations from the two sensors are separated by no more than 1 day. Moreover, in this search for doublets, we expand the number of possible matches by assuming that the angular distribution of TOA reflectances is symmetrical with respect to the principal plane.

Because an exact geometrical match is often not possible, the search for doublets is carried out by looking for acquisitions between sensor i and sensor j, satisfying the condition $\chi_{ij} < 10$, where χ_{ij} is defined as

$$\chi_{ij} = \sqrt{(\mathrm{SZA}_i - \mathrm{SZA}_j)^2 + (\mathrm{VZA}_i - \mathrm{VZA}_j)^2 + 1/4(|\mathrm{RAA}_i| - |\mathrm{RAA}_j|)^2} \quad (2)$$

The condition $\chi_{ij} < 10$ roughly corresponds to configurations for which the differences in SZAs and VZAs are less than 6°, and the differences in RAAs are less than 12°.

Moreover, if for an acquisition of sensor i, on a given day, there are several acquisitions from the sensor j satisfying the previous geometrical and temporal criteria, only the doublet with the smallest χ_{ij} is kept.

Lastly, doublets where the SZA of one of the two acquisitions is greater than 65° are discarded (see Discussion for a justification of this upper value).

Site characteristics and climatology

Dome C is located on the Antarctic Plateau at an elevation of about 3200 m above sea level at approximately 75°S, 123°E. The site is 1100 km inland from the French research station at Dumont D'Urville, 1100 km inland from the Australian Casey Station, and 1200 km inland from the Italian Zucchelli Station at Terra Nova Bay.

Because of its high latitude, space measurements in the sun-reflected part of the spectrum from optical sensors are possible only during the summer season (i.e., from October to March). The ROI chosen for intercomparison of TOA reflectances lies between 75.20°S and 75.00°S and between 123.20°E and 123.60°E.

Meteorological conditions at Dome C have been continuously measured at an automatic weather station since 1980. Atmospheric opacity, sky emission, and turbulence measurements have also been carried out. These measurements are reviewed in Lawrence et al. (2007). Atmospheric conditions are characterized by low atmospheric aerosol content, water vapour content, and cloudiness.

The surface BRDF of the site was characterized by Hudson et al. (2006).

Satellite data

The satellite data consist of L1B data (i.e., radiometrically calibrated and georeferenced TOA data) starting in 2002 and finishing in 2008 for each considered sensor.

MERIS data

The MERIS instrument provides data at two spatial resolutions: 300 m (full resolution) and 1.2 km (reduced resolution) in 15 bands centered between 412 and 940 nm. The MERIS data presented are L1B reduced resolution (i.e., approximately 1.2 km). MERIS radiometric and spectral calibration is based on onboard solar diffusers, and the instrument spectral model was further characterized in flight (Delwart et al., 2007). The data originate from the latest full reprocessing of the archive (second reprocessing).

In this study, the L1B data are further corrected for the smile effect, which refers to an across-track variable spectral shift of up to 1 nm with respect to the nominal central wavelength of each spectral band. The smile correction was restricted to the irradiance correction (see Bourg et al., 2008), as justified by the small spectral variations in surface reflectivity.

The irradiance correction was carried out and the TOA spectral radiances were converted to TOA reflectances via the mean annual extraterrestrial solar irradiance from Thuillier et al. (2003), the instrument RSR, and the correction for the Earth–Sun distance following the formulation of Gregg and Carder (1990). The latitude and longitude corrections were applied accounting for the target altitude.

The data presented in this paper cover the period from October 2002 to October 2008.

AATSR data

The AATSR is a dual-view instrument with seven channels spanning from the visible to the thermal infrared and a spatial resolution of approximately 1 km.

The calibration system for the channels in the sun-reflected spectrum (VISCAL) provides a source for calibration once per orbit, using sunlight to illuminate a diffusing plate in channels at 560, 670, and 860 nm.

AATSR L1B data are provided to users as so-called normalized radiances:

$$R^{\mathrm{TOA}} = \frac{\pi L^{\mathrm{TOA}}}{E_0} \times 100 \quad (3)$$

The conversion of normalized radiances to remote sensing reflectances only requires that the normalized radiance be divided by 100 times the cosine of the SZA.

Starting from 30 November 2005, a drift correction has been implemented in the operational data stream based on vicarious calibration from Smith et al. (2008). All previous L1B data presented in this paper have been processed to account for these drift corrections. Georeferentiation corrections accounting for the target altitude were applied.

A-MODIS data

A-MODIS provides data at a spatial resolution between 250 m and 1 km in narrow spectral bands centered between 400 nm and 13 μm. A-MODIS data presented here are L1B 1 km products from reprocessing 1.1. Similarly to AATSR, A-MODIS data are provided as normalized radiance. Their conversion into remote sensing reflectances only requires dividing the normalized radiance by the cosine of SZA. Only those spectral bands that do not saturate over Dome C in the visible spectrum are extracted. Calibration of the L1B reflective solar bands is based on an onboard solar diffuser (Xiong et al., 2003).

A number of spectral bands per sensor are available for each doublet that can be compared to those of the other sensor. **Table 1** shows the three spectral bands that have similar spectral responses for AATSR, A-MODIS, and MERIS and are thus directly comparable. The A-MODIS ocean spectral bands corresponding to the MERIS spectral bands could not be used here because their radiometric gain is such that they saturate over bright targets such as Dome C.

Results

After cloud screening of the satellite data and conversion to the remote sensing reflectance, the grand total of acquisitions over the period 2002–2008 is 553 for AATSR (each viewing geometry being considered as an acquisition), 1473 for A-MODIS, and 976 for MERIS. Cloud screening of the data resulted in discarding about 50% of the L1B data. **Figure 1** shows the time series of MERIS TOA reflectances after cloud screening at 865 nm. Seasonal variations of the reflectance are visible as well as the winter dark periods where no acquisitions are made in the visible spectral range. The TOA reflectance peaks each year at about 0.9.

By applying the previously described geometrical and temporal criteria to identify doublets of remote sensing reflectances between AATSR, A-MODIS, and MERIS, we obtain the number of doublets reported in **Table 2**.

Figures 2 and **3** show the temporal variations of the TOA reflectance differences from doublets obtained between A-MODIS and MERIS and between AATSR and MERIS, respectively.

Table 1. Spectral bands available for each sensor in this study.

Band (nm)	MODIS	AATSR	MERIS
560	×	×	×
670		×	×
860	×	×	×

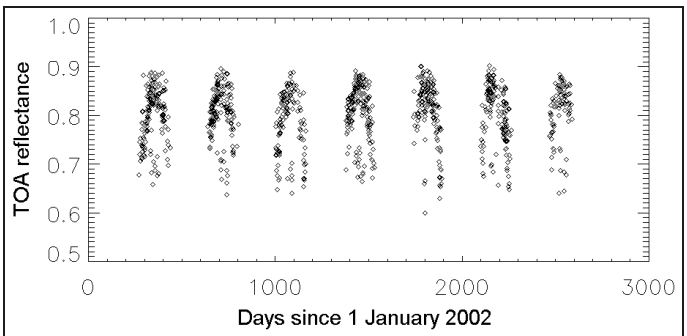

Figure 1. Time series of TOA reflectances at 865 nm from MERIS over Dome C after cloud screening between 2002 and 2009.

Discussion

In the following sections we discuss the potential sources of radiometric differences between observations from two different sensors induced by our methodology, and we try to quantify their impact where possible.

Day-to-day variability of the TOA reflectance

When comparing two acquisitions from two different sensors and made using the same geometry (within the $\chi_{ij} < 10$ criteria) but 1 day apart, we might introduce a random difference between the two TOA reflectances owing to day-to-day variability of the surface–atmospheric BRDF variability. We have tested a more stringent temporal matching criterion, namely that acquisitions from the two sensors should be done for the same day. This resulted in a reduction in the number of doublets, as expected. This also resulted in mean TOA reflectance differences below 0.3% when averaged over the period 2002–2008 between MERIS and A-MODIS at 560 and 860 nm. The effect of day-to-day variability of the atmosphere–surface spectral and direction properties thus appears marginal.

Sensitivity of the methodology to the angular matching criteria χ_{ij}

The choice of an upper value of 10 for the χ_{ij} criterion is driven by a trade-off between having a sufficient number of doublets to statistically compare the radiometry from two

Table 2. Number of doublets identified between the sensors, with $\chi_{ij} < 10$ and SZA $< 65°$ at 865 and 560 nm.

	A-MODIS	AATSR	MERIS
A-MODIS		21 (154)	41 (326)
AATSR	21 (154)		12 (24)
MERIS	41 (326)	12 (24)	

Note: The number of doublets obtained with $\chi_{ij} < 10$ and no restriction on the SZA is given in parentheses.

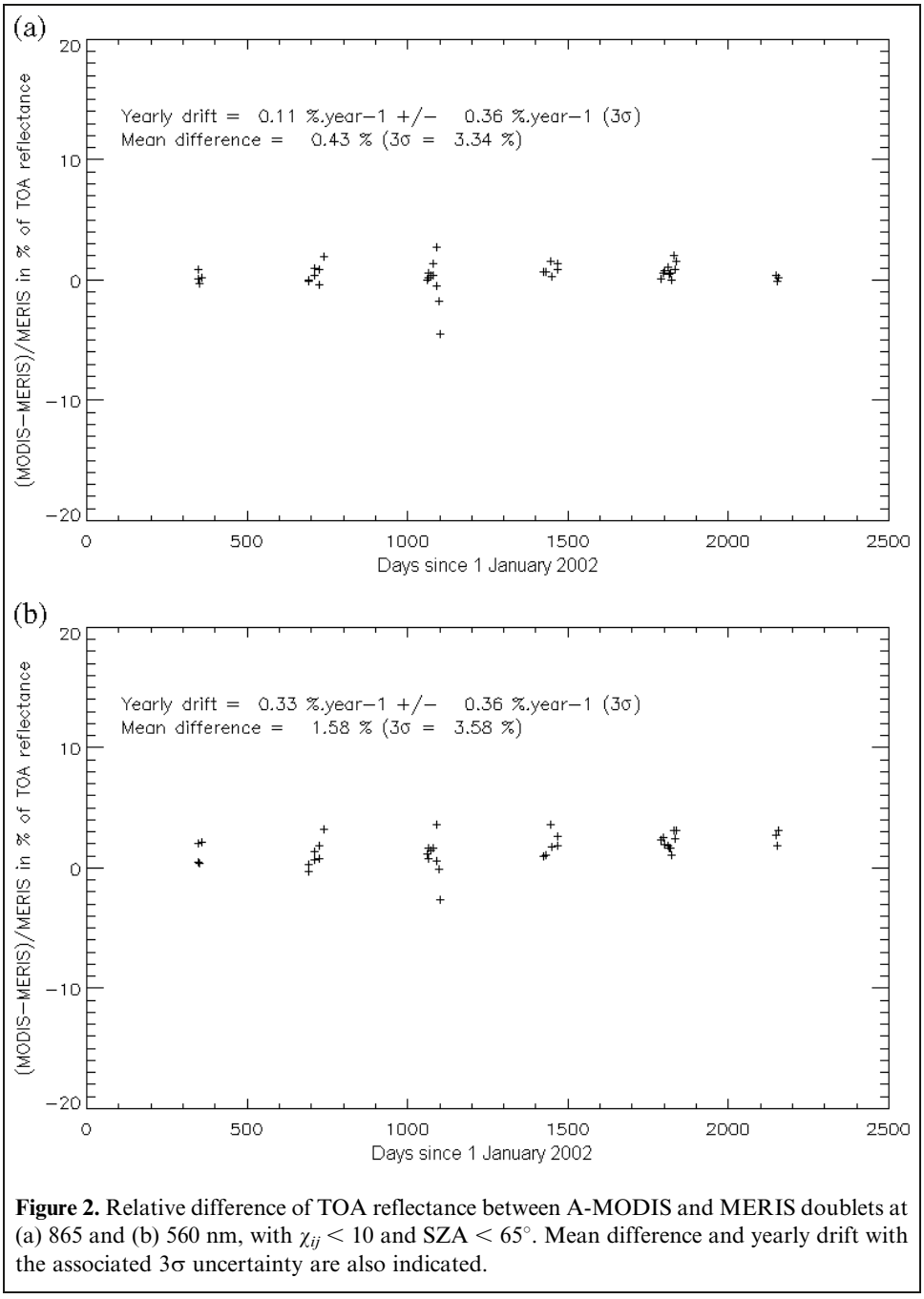

Figure 2. Relative difference of TOA reflectance between A-MODIS and MERIS doublets at (a) 865 and (b) 560 nm, with $\chi_{ij} < 10$ and SZA $< 65°$. Mean difference and yearly drift with the associated 3σ uncertainty are also indicated.

sensors and minimizing the influence of the non-Lambertian TOA BRDF. In our sensitivity analysis of this upper value of χ_{ij}, we find that a lower value only results in fewer doublets and no significant change in the computation of statistical indicators characterizing the relative TOA reflectance differences between sensors.

On the validity of the assumption of symmetry of the TOA BRDF with respect to the principal plane

The underlying assumption of our methodology is that the TOA reflectance BRDF is symmetrical with respect to the principal plane. Most doublets between MERIS and A-MODIS are obtained under this assumption.

Such an assumption should hold as long as there is no azimuth-dependent structure on the surface. Warren et al. (1998) show that the wind-driven sastrugi has a significant effect on the BRDF at the South Pole station. The BRDF measurements at Dome C and modelling presented in Hudson et al. (2006) were, however, carried out assuming invariance of the BRDF with respect to the azimuth of the sun and are parameterized by the RAA rather than the viewing azimuth and sun azimuth angles taken separately. Hudson et al. state that such invariance is justified by the lack of azimuth orientation in surface roughness patterns due to the weakness and lack of directional consistency of winds at Dome C; they further tested this assumption with their measurements by

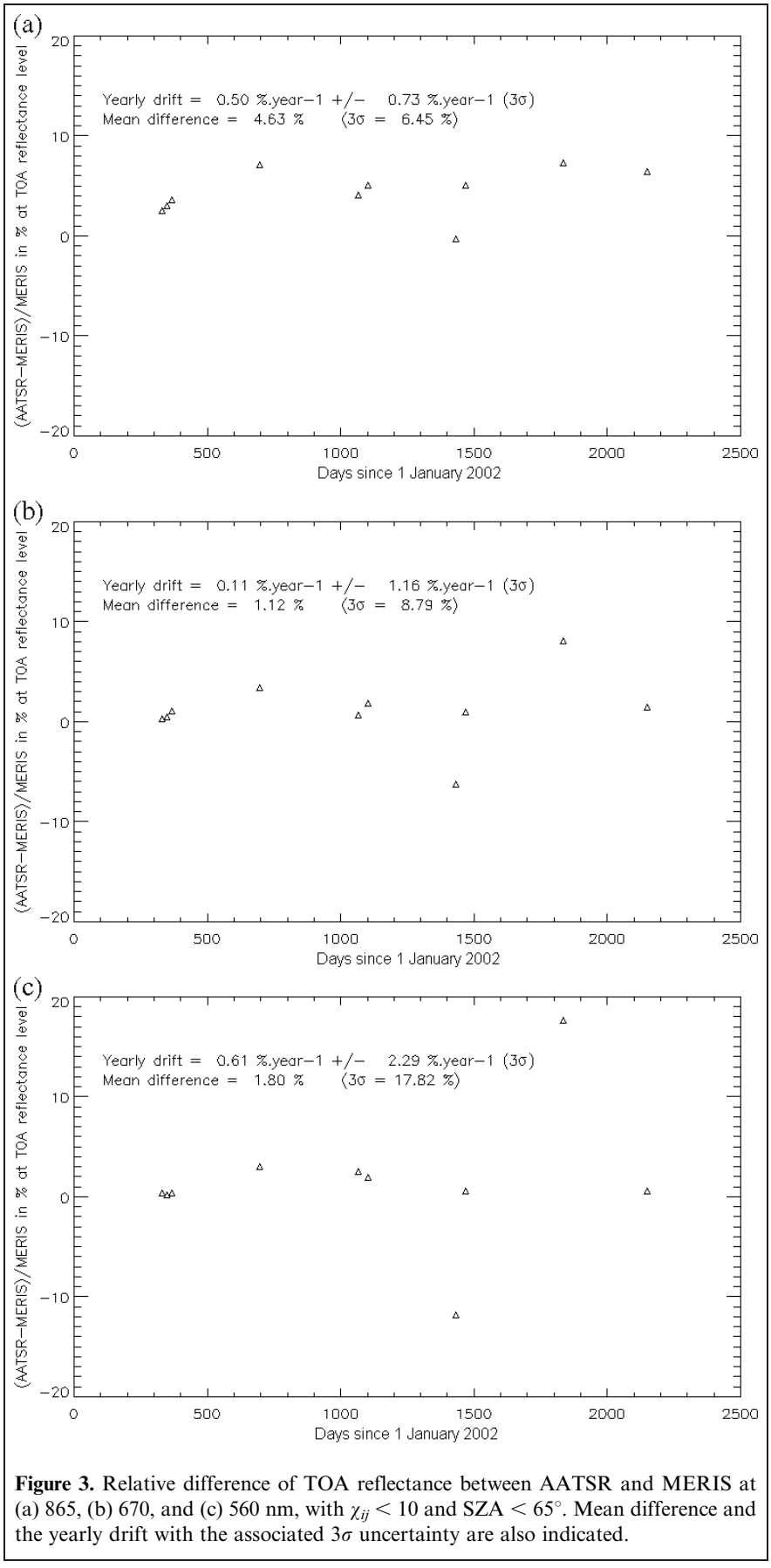

Figure 3. Relative difference of TOA reflectance between AATSR and MERIS at (a) 865, (b) 670, and (c) 560 nm, with $\chi_{ij} < 10$ and SZA $< 65^{\circ}$. Mean difference and the yearly drift with the associated 3σ uncertainty are also indicated.

comparing pairs of observations made at RAAs symmetric across the principal plane for wavelengths below 1400 nm. Hudson et al. report differences generally less than 5% that were not related to the RAA or to the VZA. Moreover, they found a root mean square error (RMSE) of 3% between their BRDF model (assuming symmetry across the principal plane) and the measurements. Warren et al. (1998) report that such differences are related to the RAA and VZA when sastrugi are present and have a significant impact on the symmetry across the principal plane. Hudson et al. (2006) suggest that the measured differences across the principal plane are due to various sources of noise in their measurements rather than an actual lack of symmetry across the principal plane. At surface BRDF level, we can conclude that the assumption of symmetry across the principal plane appears confirmed by the Hudson et al. observations at Dome C with an RMSE of less than 3%. Since we have only selected clear sky scenes, no asymmetry with respect to the principal plane can be expected from the atmospheric contribution to the TOA signal. We thus expect this principle of symmetry to be valid to better than 3% RMSE at TOA level (surface reflectance is the main contributor to the TOA reflectance). Assuming a normal distribution of the random error between the Hudson et al. BRDF parameterization and measurements, their 3% RMSE can be translated into a potential bias induced by the lack of symmetry across the principal plane of less than 1% when comparing more than 10 doublets of observations (the bias is the uncertainty to the mean difference and is the RMSE divided by the square root of the number of doublets).

Sensitivity of the methodology to the upper value of the SZA: the choice of 65° as the upper value for doublet selection

We find that including doublets of acquisitions done with increasing SZA results in an increase of the uncertainty of the methodology: the difference between two sensor measurements increases with an increase in SZA. This is illustrated in **Figure 4**, where we have not restricted the search for doublets to any specific SZA for MERIS and A-MODIS. Such an increase can be explained by the measurements carried out by Hudson et al. (2006), which show a general increase in nonisotropy of the Dome C surface BRDF with an increase in SZA. Such anisotropy results in more pronounced radiometric differences with an increase in SZA for acquisitions separated by a given angular distance.

From **Figure 4** we calculate that restricting the SZA to values less than 65° allows uncertainties induced by such BRDF effect to be kept at less than 2% (standard deviation). It is worth noting that such sensitivity of the methodology to the SZA variations mostly results in a random uncertainty for SZA values less than 65° and marginally in a systematic uncertainty.

These considerations motivated our choice of 65° as the maximum value of SZA when selecting the doublets of observations between sensors.

Differences in TOA reflectances induced by differences in RSR between sensors

The RSR of each instrument overlaps for most bands, but noticeable differences can be observed. To simulate the differences at TOA reflectance level induced by the sensor-to-sensor differences in RSR, a synthetic spectrum of Dome C is generated (**Figure 5**). This spectrum is generated using the libRadtran radiative transfer toolbox developed by Mayer and Kylling (2005). We simulate the TOA reflectance spectrum for a nadir-looking geometry, with a surface of spectrally constant reflectance of 0.9, located at an altitude of 3200 m, beneath a US 1976 standard atmosphere, in aerosol-free conditions, with a sun zenith angle of 65° and a nadir viewing angle. The choice of a US 1976 atmospheric profile, characterized by significant water vapour content and ozone content and the highest SZA, is a conservative case when trying to estimate TOA reflectance differences induced by differences in RSR and gaseous absorption.

The TOA band average reflectances are computed from the synthetic reflectance spectrum to assess the impact of atmospheric absorption spectral features in each band and for each sensor. **Table 3** shows that in all bands, we can expect sensor-to-sensor systematic differences due to RSR differences of less than 1% in TOA reflectance.

Sensitivity of the methodology to the accuracy of the geolocalization

AATSR, A-MODIS, and MERIS were specified to generate L1B data with geolocalization errors less than the 2 km scale. The geolocalization errors are, in fact, claimed to be within a few hundred metres for MERIS and MODIS full-resolution data (e.g., for MERIS see Goryl and Saunier, 2004). For each A-MODIS, AATSR, and MERIS scene, the TOA reflectances are extracted from a fixed ROI. To assess the impact of potential geolocalization errors on the TOA reflectances, theROI was shifted by about 2 km north and east on a MERIS scene. The differences between the TOA spectral reflectances of the shifted ROI and those of the nonshifted ROI remain below 0.5% in all spectral bands. The Dome C area is radiometrically spatially uniform; the relative standard deviation of the TOA reflectance within our ROI is below 0.5% in all bands.

Systematic and random TOA reflectance differences between two sensors

When assessing the uncertainties associated with the methodology, we should attempt to distinguish between the potential sources of systematic and random uncertainties.

The identified sources of systematic uncertainties are (1) those linked to the differences in spectral response ($<1\%$), (2) those related to a systematic difference in geolocalization ($<0.5\%$), and (3) those related to the lack of symmetry across the principal plane ($<1\%$). These three errors combined might thus induce systematic uncertainties of less than 3%.

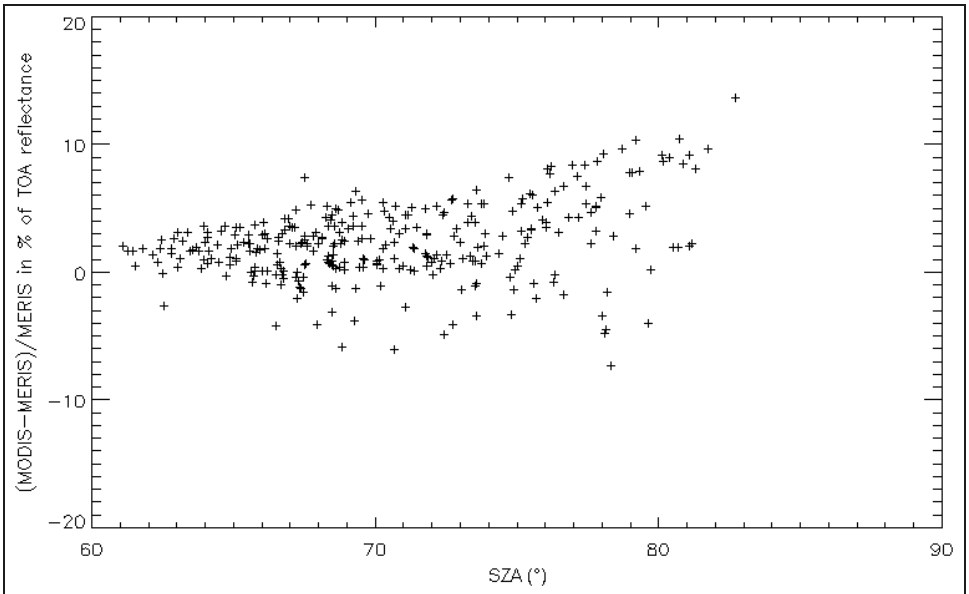

Figure 4. Relative difference of TOA reflectance between A-MODIS and MERIS doublets as a function of SZA at 560 nm, where $\chi_{ij} < 10$.

The identified sources of random uncertainties are (1) the nonexact angular matching between acquisitions (<2%), (2) the nonexact temporal matching between acquisitions (<2%), (3) the random uncertainties induced by the departure of the TOA BRDF from our assumption of symmetry with respect to the principal plane (<3%), (4) the random effects of geolocalization differences (<0.5%), and (5) the random effects of the RSR differences (governed by H_2O and O_3

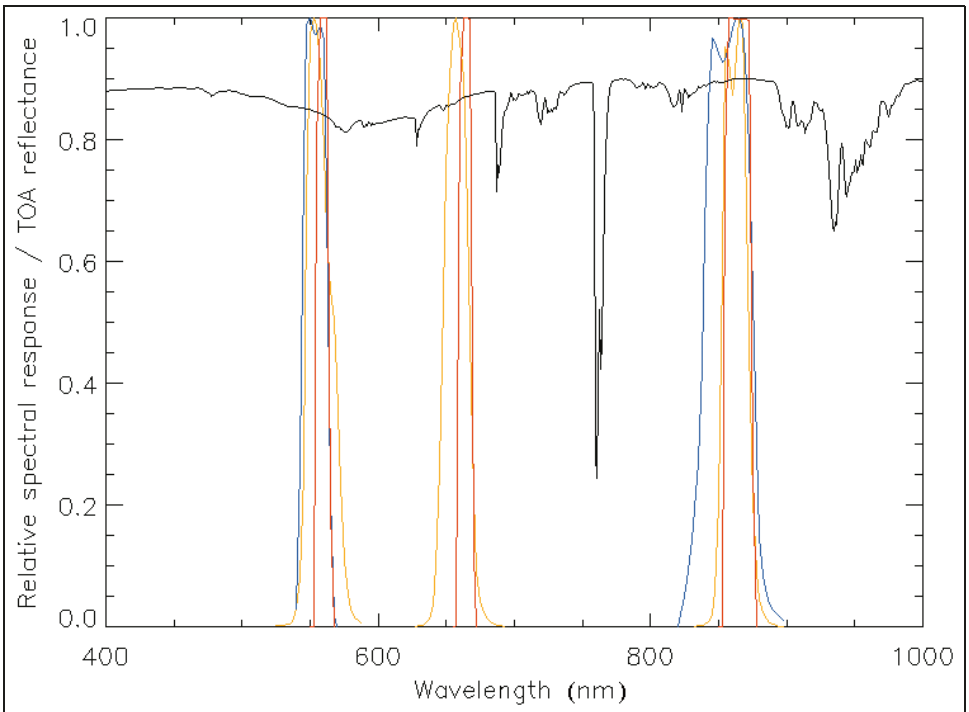

Figure 5. TOA reflectance spectrum (black line) simulated with libRadtran for a nadir-looking geometry, with a surface of spectrally constant reflectance of 0.9, located at an altitude of 3200 m, beneath a US 1976 standard atmosphere, in aerosol-free conditions, with a sun zenith angle of 65° and a nadir viewing angle. Superimposed are MERIS (red line) and AATSR (orange line) spectral responses at 560, 670, and 870 nm. The blue line denotes A-MODIS spectral responses at 560 and 870 nm.

Table 3. Simulated band-averaged TOA reflectance for MERIS and differences for A-MODIS and AATSR relative to MERIS.

Band (nm)	MERIS TOA reflectance	A-MODIS TOA difference relative to MERIS (%)	AATSR TOA difference relative to MERIS (%)
560	0.840	−0.4	0.0
670	0.869		0.7
860	0.898	0.3	0.0

Note: The simulation was obtained with the instrument RSRs and a libRadtran simulation for a nadir-looking sensor observing a surface with a spectrally constant reflectance of 0.9, located at an altitude of 3200 m, beneath a US 1976 standard atmosphere, in aerosol-free conditions, with a sun zenith angle of 65°.

variability) (<1%). The ideal way to evaluate the total random uncertainty of the methodology would be to compare two perfectly well calibrated instruments whose measurements are not affected by random errors. The total random uncertainty of the methodology would then be accessed using as a proxy the standard deviation of the mean difference between the TOA reflectances from these two sensors. Looking at the results from the comparison between MERIS and A-MODIS in **Figure 2**, we can actually get an upper estimate of the random uncertainty of the methodology of less than 2% ($3\sigma < 4\%$). This is an upper estimate because it includes a random component from the MERIS and A-MODIS measurements themselves and the random uncertainty of the methodology.

Such random uncertainty of the methodology can be statistically removed when averaged over a sufficiently large number of doublets, for example if computing the mean difference in TOA reflectance between two sensors. The only remaining uncertainty is the systematic uncertainty of the methodology (<3%).

Comparison of TOA reflectances from A-MODIS, AATSR, and MERIS

In light of the previous discussion, the methodology presented here provides the means to identify systematic radiometric calibration differences greater than 3%. **Figure 2** shows the relative differences in TOA reflectance between MERIS and A-MODIS. These sensors are in agreement within the systematic uncertainty of the methodology at both 560 and 865 nm. **Figure 3** shows the relative differences in TOA reflectance between MERIS and AATSR. Outliers are due to regular short periods (2 days every 3 months) of warming of the AATSR instrument to allow outgassing, which results in rapid changes in sensitivity of the instrument. These events become more visible when looking at a comparison of the reflectances from MODIS and AATSR (not shown in the figures). If these outliers are removed, the comparison of MERIS and AATSR shows agreement within the systematic uncertainty of the methodology at 560 and 670 nm. The results at 870 nm seem to indicate a significant difference in radiometry of 4% between MERIS and AATSR. This result is confirmed when comparing A-MODIS and AATSR.

Conclusion

The methodology presented in this paper allows direct comparison between measurements from sensors onboard different platforms, directly at TOA and without any atmospheric correction. The methodology identifies systematic radiometric differences between two sensors with a systematic uncertainty estimated to be less than 3% and a random uncertainty of less than 2% standard deviation over Dome C. These values are of the same order as the best absolute radiometric calibration uncertainties for Earth Observation sensors. Dome C appears to be a relevant site to apply such methodology as long as geometries with large SZA (>65°) are avoided. One of the limitations of the methodology is that its uncertainty increases with an increase in BRDF nonisotropy. It is thus more suited to surface types with slowly variable BRDFs and might not be applicable to observational cases such as a water surface in sun-glint geometry. The applicability of this methodology is, however, not restricted to high-latitude locations or to nadir observations (as is the case in the comparable SNO methodology for polar-orbiting satellites), and it can be (and has been) applied to sites at any latitude and to other surface types.

This methodology, when applied over Dome C, indicates that the MERIS and A-MODIS data are in radiometric agreement within 3%. The AATSR data do not appear to be in line with those from MERIS and A-MODIS at 860 nm within 4%.

Acknowledgements

MODIS data were obtained from the National Aeronautics and Space Administration (NASA) Langley Research Center – Atmospheric Sciences Data Center. AATSR and MERIS data were provided by the European Space Agency. We would like to thank the reviewers for their comments, which contributed to clarifying this paper.

References

Bourg, L., D'Alba, L., and Colagrande, P. 2008. *MERIS SMILE effect characterisation and correction*. European Space Agency, Paris. Technical note. Available from http://earth.esa.int/pcs/envisat/meris/documentation/MERIS_Smile_Effect.pdf.

Bouvet, M. 2006. Intercomparison of imaging spectrometers over the Salar de Uyuni (Bolivia). In *Proceedings of the Second Working Meeting on MERIS and AATSR Calibration and Geophysical Validation (MAVT-2006)*, 20–24 March 2006, Frascati, Italy. Edited by D. Danesy. European Space Agency, Paris. ESASP-615.

Cabot, F., Hagolle, O., Ruffel, C., and Henry, P. 1999. Remote sensing data repository for in-flight calibration of optical sensors over terrestrial targets. In *Earth Observing Systems IV*, 18–20 July 1999, Denver, Colo. Edited by W.L. Barnes. SPIE, Bellingham, Wash. Proceedings of SPIE Vol. 3750, pp. 514–523.

Cao, C., Weinreb, M., and Xu, H. 2004. Predicting simultaneous nadir overpasses among polar-orbiting meteorological satellites for the intersatellite calibration of radiometers. *Journal of Atmospheric and Oceanic Technology*, Vol. 21, pp. 537–542.

Chandrasekhar, S. 1960. *Radiative transfer*. Dover Publications, Inc., New York.

Delwart, S., Preusker, R., Bourg, L., Santer, R., Ramon, D., and Fischer, J. 2007. MERIS in-flight spectral calibration. *International Journal of Remote Sensing*, Vol. 28, No. 3–4, pp. 479–496.

Goryl, P., and Saunier, S. 2004. *Analysis of the absolute location accuracy of MERIS FR (full resolution) level 1B products*. European Space Agency, ESRIN, Paris. Technical Report 15993/02/I-LG. Available from http://earth.esa.int/pcs/envisat/meris/documentation/GAEL-P179-TCN-006-01-00-Meris_Absolute_location_control_report.pdf.

Gregg, W., and Carder, K.L. 1990. A simple spectral solar irradiance model for cloudless maritime atmospheres. *Limnology and Oceanography*, Vol. 35, No. 8, pp. 1657–1675.

Hudson, S.R., Warren, S.G., Brandt, R.E., Grenfell, T.C., and Six, D. 2006. Spectral bidirectional reflectance of Antarctic snow: measurements and parameterization. *Journal of Geophysical Research*, Vol. 111, D18106. doi:10.1029/2006JD007290.

Isaacman, A., Toller, G., Guenther, B., Barnes, W.L., and Xiong, X. 2003. MODIS Level 1B calibration and data products. In *Earth Observing Systems VIII*, 3–6 August 2003, San Diego, Calif. Edited by W.L. Barnes. SPIE, Bellingham, Wash. Proceedings of SPIE Vol. 5151, pp. 552–562.

Lawrence, J.S., Ashley, M.C.B., Burton, M.G., and Storey, J.W.V. 2007. Dome C's atmospheric conditions: implications for astronomy. *Chinese Astronomy and Astrophysics*, Vol. 31, pp. 221–227.

Mayer, B., and Kylling, A. 2005. Technical note: The libRadtran software package for radiative transfer calculations — description and examples of use. *Atmospheric Chemistry and Physics*, Vol. 5, pp. 1855–1877.

Smith, D., Poulsen, C., and Latter, B. 2008. Calibration status of AATSR and MERIS reflectance channels. In *Proceedings of the MERIS AATSR Validation Team Workshop 2008*, 21–26 September 2008, Frascati, Italy. European Space Agency, Paris.

Thome, K.J., Helder, D.L., Aaron, D., and Dewald, J.D. 2004. Landsat-5 TM and Landsat-7 ETM+ absolute radiometric calibration using the reflectance-based method. *IEEE Transactions on Geoscience and Remote Sensing*, Vol. 42, pp. 2777–2785. doi:10.1109/TGRS.2004.839085.

Thuillier, G., Hersé, M., Simon, P.C., Labs, D., Mandel, H., Gillotay, D., and Foujols, T. 2003. The solar spectral irradiance from 200 to 2400 nm as measured by the SOLSPEC spectrometer from the ATLAS 1-2-3 and EURECA missions. *Solar Physics*, Vol. 214, No. 1, pp. 1–22.

Tinel, C. 2006. Vicarious calibration over deserts sites.In *Proceedings of the Second Working Meeting on MERIS and AATSR Calibration and Geophysical Validation (MAVT-2006)*, 20–24 March 2006, Frascati, Italy. Edited by D. Danesy. European Space Agency, Paris. ESASP-615.

Vermote, E., Santer, R., Deschamps, P.Y., and Herman, M. 1992. In-flight calibration of large field of view sensors at short wavelengths using Rayleigh scattering. *International Journal of Remote Sensing*, Vol. 13, pp. 3409–3429.

Warren, S.G., Brandt, R.E., and Hinton, P. 1998. Effect of surface roughness on bidirectional reflectance of Antarctic snow. *Journal of Geophysical Research (Planets)*, Vol. 103, pp. 25 789 – 25 807.

Xiong, X., Chiang, K., Esposito, J., Guenther, B., and Barnes, W.L. 2003. MODIS on-orbit calibration and characterization. *Metrologia*, Vol. 40, pp. 89–92.